Full-duplex or Half-duplex: A Bayesian Game for Wireless Networks with Heterogeneous Self-interference Cancellation Capabilities

Wessam Afifi*, *Member, IEEE,* Mohammad J. Abdel-Rahman*, *Member, IEEE,*
Marwan Krunz, *Fellow, IEEE,* and Allen B. MacKenzie, *Senior Member, IEEE*
*Co-first Authors

Abstract—Recently, tremendous progress has been made in self-interference cancellation (SIC) techniques that enable a wireless device to transmit and receive data simultaneously on the same frequency channel, a.k.a. in-band full-duplex (FD). Although operating in FD mode significantly improves the throughput of a single wireless link, it doubles the number of concurrent transmissions, which limits the potential for coexistence between multiple FD-enabled links. In this paper, we consider the coexistence problem of concurrent transmissions between multiple FD-enabled links with different SIC capabilities; each link can operate in either FD or half-duplex mode. First, we consider two links and formulate the interactions between them as a Bayesian game. In this game, each link tries to maximize its throughput while minimizing the transmission power cost. We derive a closed-form expression for the Bayesian Nash equilibrium and determine the conditions under which no outage occurs at either link. Then, we study the coexistence problem between more than two links, assuming that each link is only affected by its dominant interfering link. We show that under this assumption no more than two links will be involved in a single game. Finally, we corroborate our analytical findings via extensive simulations and numerical results.

Index Terms—In-band full-duplex, self-interference cancellation, coexistence, Bayesian game, full-duplex wireless networks.

1 Introduction

Classical wireless systems achieve bidirectional communications by separating the forward and reverse links in time, i.e., time division duplexing (TDD), or frequency, i.e., frequency division duplexing (FDD). Some wireless systems, such as 4G LTE, support both schemes (e.g., LTE-TDD and LTE-FDD). The challenge of achieving simultaneous transmission and reception on the same frequency channel, i.e., in-band full-duplex (FD), is related to the strong self-interference that arises when a device that is receiving an information signal attempts to transmit another signal at the same time [2]. Because of path loss, the received power of the intended signal from the peer node is often much weaker than the node's self-interference. This results in saturating the analog-to-digital converter (ADC) and prevents packet decoding. Recently, new designs for analog and digital self-interference cancellation (SIC) techniques have been proposed (see [3, 4] for a survey), which together provide up to 110 dB SIC on a single-antenna FD transceiver [5].

W. Afifi and M. Krunz are with the Department of Electrical and Computer Engineering, University of Arizona, Tucson, AZ 85721 USA e-mail: wessamafifi@email.arizona.edu and krunz@email.arizona.edu.
M. J. Abdel-Rahman was with the Department of Electrical and Computer Engineering, Virginia Polytechnic Institute and State University, Blacksburg, VA 24060 USA. He is now with the School of Computer Engineering and Informatics, Al Hussein Technical University (HTU), Amman, Jordan.
A. B. MacKenzie is with the Department of Electrical and Computer Engineering, Virginia Polytechnic Institute and State University, Blacksburg, VA 24060 USA.
A preliminary version of this paper was presented at the WiOpt Conference, May 2016 [1].

From one link's perspective, the advantage of in-band FD communications is clear; it basically doubles the link's throughput. However, such gain is less obvious in the case of a network of multiple interfering links. When these links operate in the same vicinity (i.e., the same collision domain), it is not always optimal for all links to operate in FD mode [4]. To illustrate, consider the three scenarios in Figure 1. In each scenario, two links are active at the same time and over the same frequency channel. According to the scenario in Figure 1(a), transmitting in an HD fashion enables both links $a \rightarrow b$ and $c \rightarrow d$ to operate simultaneously over the same channel, achieving a total throughput of $2R$ bps (For simplicity, in this example we assume that all transmissions are associated with a constant rate R). However, if link $a \rightarrow b$ switches unilaterally from HD to FD, as shown in Figure 1(b), collisions may occur at both nodes a and d, reducing the network throughput to R bps (only $a \rightarrow b$ transmission is successful). One reason for the collision at node a is that the SINR at node a becomes lower than the SINR threshold (which is function of the modulation and coding scheme used) needed for successful decoding of the message from node b. Under the assumed path-loss model, the occurrence of this scenario depends mainly on the distances between nodes a and b, and between nodes a and c.

If link $c \rightarrow d$ switches to FD mode instead of $a \rightarrow b$, the same argument used in the previous case applies. If both links operate in FD mode, collisions will occur at all four nodes, reducing the network throughput to zero (see Figure 1(c)). Note that this is a simplified example of a small network with only two links. The situation worsens with more interfering links.

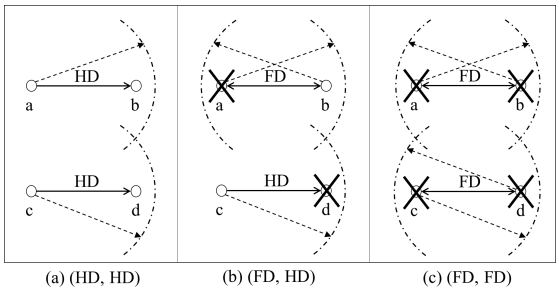

Fig. 1. Implications of operating wireless networks in FD fashion. (a) (HD, HD) strategy achieves a total throughput of $2R$ bps, (b) (FD, HD) strategy achieves R bps, while (c) (FD, FD) strategy achieves zero throughput. The arcs represent the transmission ranges of different nodes.

Most existing literature that studies the performance of FD networks assume perfect SIC (A detailed discussion of the related work is given in Section 2). In [6] the authors proposed stochastic resource allocation schemes for LTE networks with *heterogeneous* (perfect and imperfect) SIC capabilities. These schemes are centralized and exhibit high computational complexity. In this paper, we develop a game-theoretic framework to analyze the performance of wireless networks with heterogeneous SIC capabilities and in the absence of any global information, i.e., a link does not know the exact SIC capability of its neighboring link. The key idea is to allow nodes to determine, in a distributed fashion, the optimal operation mode (FD or HD). Such a distributed approach is critical to many wireless networks, including heterogeneous networks that coexist on the same band, e.g., LTE and Wi-Fi that operate on the unlicensed 5 GHz bands [7]. In these scenarios, it is unlikely to have collaboration between the Wi-Fi AP and the LTE-U/LAA HeNB such that they know the exact SIC of each other. This applies even if the network is small (e.g., coexistence between a single Wi-Fi link and a single LTE-U/LAA link).

The contributions of this paper can be summarized as follows:

1) We analyze a simple (HD vs. FD) game between two bidirectional links to gain insight into the coexistence problem. In this game, links (players) know the exact SIC capabilities of each other. Simple utilities and interference models are considered. We find that the outcome of this game depends on the residual self-interference (RSI) (due to imperfect SIC) and external interference (from one link on the other).
2) To capture the heterogeneity in SIC capabilities, we then formulate a Bayesian game between the two links. In this game, the SIC capability of each link specifies its 'type,' which is unknown to the other link. We derive the Bayesian Nash equilibrium (BNE) for this game. From our analysis, we observe that the range of possible SIC values a given player may take can be divided into three regions (types). In two types, either the HD or the FD strategy is dominant, while the BNE in the third type depends mainly on the probability distribution of the other player's types. The thresholds that specify the regions of various SIC types depend, among other factors, on the outage probabilities of the player's forward and reverse links. Accordingly, we derive closed-form expressions for these thresholds under different outage scenarios.
3) To capture the interactions between more than two links, we consider a network of FD-enabled links with heterogeneous SIC capabilities and study the coexistence problem. Analyzing the Bayesian game for more than two links is very complex and intractable due to the mutual dependence between players' actions and the fact that the exact SICs of players are unknown. Hence, we study the multi-player Bayesian game under the simplifying assumption that every player is mainly affected by a single dominating link.
4) Finally, we corroborate our analytical findings via extensive simulations and numerical results.

The rest of the paper is organized as follows. We discuss some related works in Section 2 and describe the simple two-player strategic game in Section 3. The Bayesian game is formulated and analyzed in Section 4. In Section 5, we extend the two-player Bayesian game to more than two links. The proposed games are simulated in Section 6. Finally, in Section 7 we conclude the paper and provide directions for future research.

2 Related Work

There are several efforts in the literature that studied and demonstrated the feasibility of FD communications from one link's perspective [5, 8–13]. The feasibility of network-wide FD communications was discussed in [14–21]. In [14], the authors analyzed the outage probability for FD-based cellular systems based on two schemes: Bidirectional FD communications between the base station (BS) and the user equipment (UE) and three-node scheme (the BS transmits to a UE while simultaneously receiving from another UE). The authors found that the three-node scheme has better performance and is more practical than the two-node scheme if the RSI signal is relatively high. The authors in [15] theoretically studied the benefits of FD communications for multi-hop networks by computing the achievable end-to-end throughput. They showed that in some scenarios, the benefits of FD communications in multi-hop networks can exceed double that of HD networks.

In [16] the authors studied the multiplexing gain offered by FD communications in multi-cell networks. In addition to RSI, the authors considered the interference from uplink nodes on the reception of the downlink nodes (assuming a three-node setting). To remedy this interference, the authors considered a solution based on spatial interference alignment. In [17], the authors proposed an analytical framework to analyze the capacity gain of FD networks, assuming a CSMA-based MAC protocol. They found that spatial reuse and inter-link interference may cause significant reduction to network capacity. To enable FD Wi-Fi networks, the authors in [18] proposed a MAC protocol and presented an experimental and simulation study to assess the performance of their scheme. In contrast to [17], they found that FD communications can potentially enhance the performance of Wi-Fi networks. The authors in [20] considered the inter-node interference in a three-node (base station, downlink node, and uplink node) FD OFDM network. To maximize

the network sum-throughput for this scenario, they proposed different power allocation schemes while taking into account inter-node interference.

Game theory has been used to study FD wireless networks [22–26]. In [22], the authors discussed several game theoretic models, including evolutionary games used for adaptive mode switching problems, auction-based models used for power allocation problems, and matching theory used for subcarrier allocation. For distributed FD networks, the authors discussed non-cooperative games used for power control, matching games used for opportunistic channel assignment, and coalition games used for collaborative spectrum sensing. In [23], the authors considered virtualization in FD relay cellular networks, where they used a three-stage Stackelberg game to model a resource management problem. In [24], the authors proposed a cooperative game to solve the hidden-node problem in FD-enabled cognitive radio networks. Specifically, they exploited the possibility of simultaneous transmission and sensing on the same channel using SIC techniques. In [26], the authors proposed an adaptive FD/HD mode switching based on the residual self-interference and channel conditions to maximize the ergodic capacity. The above mentioned game-theoretic studies did not account for the heterogeneity and imperfectness in the SIC capabilities.

The achievable throughput of FD MIMO networks was investigated in [19, 21]. In [19] the authors considered a binary interference model of a general network topology and derived the conditions under which different technologies (MIMO, multi-user MIMO, and FD communications) achieve the best performance. In [21] the authors considered the problem of power minimization in an FD MIMO network subject to rate demands. They derived conditions under which the FD mode outperforms the HD mode. In [27], the authors considered MIMO FD relay systems, and specifically amplify-and-forward (AF) cooperative networks. They proposed a joint precoding/decoding system that maximizes the end-to-end system performance while reducing complexity. In [28], the authors proposed a joint transceiver design algorithm for the FD k-pair MIMO interference channel with simultaneous wireless information and power transfer. Using optimization theory, they analyzed two problems: The sum-power minimization problem and the sum-rate maximization problem. In [29–32], the authors investigated the incorporation of SIC techniques in opportunistic spectrum access (OSA) systems. In overlay models, secondary users (SUs) operate in either FD mode or simultaneous transmit-sense mode. On the other hand, in an underlay OSA network, SUs operate in either HD or FD mode. The authors in [29–32] determined the optimal operating mode for both overlay and underlay settings. Our work is different since it has different objectives and follows a different approach.

In [33], the authors proposed several stochastic formulations to minimize the cost of composing a virtual LTE-U network from a hybrid set of HD/FD Wi-Fi access points (APs). An AP is assumed to be either HD or FD (with perfect SIC). In general, different devices in a network may have different SIC capabilities, mainly depending on the employed analog/digital cancellation mechanisms. In [6] the authors proposed joint channel and BS stochastic allocation schemes for opportunistic LTE networks with heterogeneous SIC capabilities at different BSs. The resource allocation schemes in [6, 33] are centralized with high computational complexity. Instead, in this paper we develop a game-theoretic framework to analyze the performance of wireless networks with heterogeneous SIC capabilities and in the absence of any global information (i.e., a link does not know the exact SIC level of its neighboring link).

Stochastic geometry has been used in the literature to model FD-enabled wireless networks and assess their performance [34, 35]. The authors in [34] developed a spatial stochastic framework to study the tradeoff between network throughput (i.e., FD operation) and spatial reuse for CSMA-based networks. They analyzed the FD gain as a function of link distance, interference range, network density, and carrier sensing schemes. In [35] the authors studied the network capacity under the FD mode using stochastic geometry. They found that the aggregated interference is the main challenge for scalable FD networks. A unique feature of our scheme is the consideration of imperfect SIC, where nodes are unaware of other nodes SIC capability, which directly affects the optimal operation mode. In [1], we studied the coexistence problem between *two* FD-enabled wireless links with heterogeneous SIC capabilities. We formulated the problem as a two-player Bayesian game and analyzed the performance at the BNE. In this paper, we extend our study and simulations to more than two coexisting FD-enabled links.

3 Simple Normal-Form HD vs. FD Game

In this section, we study a simple strategic game between two coexisting links to identify their stable operating modes. For now, we assume that the two players (links) know all the parameters of the game, including the SIC capability of the other player. Furthermore, we consider simple utility functions and interference models. The game can be defined in the strategic form as $\mathcal{G}_s = (\mathcal{P}, \mathcal{S}, \mathcal{U})$, where $\mathcal{P} = \{P_1, P_2\}$ is the set of players, $\mathcal{S} = \{S_1, S_2\}$ is the set of strategies, and $\mathcal{U} = \{U_1, U_2\}$ is the set of utilities for the two players. For $i = 1, 2$, the strategy set $S_i = \{\text{FD, HD}\}$ is the set of pure strategies of P_i. Let a and b be the two nodes associated with P_1, and let c and d be the two nodes associated with P_2.

An FD strategy of a given player P_i indicates that both nodes of that player/link will transmit simultaneously on the same channel. On the other hand, under an HD strategy, only a single node of player P_i will transmit data to its peer. For simplicity, we assume that under the HD strategy, the transmitter are nodes a and c in case of P_1 and P_2, respectively. In practice, there will be a contention phase before the game starts, where each link decides the direction of the HD communications in the game (e.g., a to b or b to a for P_1 and similarly for P_2). To capture this contention phase, we designate the nodes of each link as *master* and *slave*. A master node is the initiator of the communications. Based on the MAC-queue lengths at both nodes, the master node decides whether communication under the HD strategy will be in the forward or reverse direction. The slave node can piggyback the value of the queue length in the ACK packet to help the master node in the selection of the communications direction.

The utilities $\mathcal{U} = \{U_1, U_2\}$ of the two links represent their respective throughputs under given strategies and hence their operating modes at the Nash equilibrium (NE), depend on two factors: External interference from one link on the other and residual self-interference. The amount of external interference depends on the channel gains and transmission powers, whereas self-interference is function of the SIC capabilities. Let R be the throughput of a link in one direction when the communication is successful. Table 1 shows two instances of the game $\mathcal{G}_s$. In the first instance (Table 1(a)), both external and self-interference are assumed to be high. As a result, if both P_1 and P_2 operate in the FD mode, then their utilities will be zero. Although (FD, FD) is a NE, it is not an efficient one. Moreover, (FD, FD) is not a unique NE. Specifically, (FD, HD) and (HD, FD) are also NEs and, in fact, they are Pareto-efficient. In another instance of $\mathcal{G}_s$ (shown in Table 1(b)), the external interference is low and all nodes have perfect SIC. In this case, (FD, FD) is an efficient and unique NE.

TABLE 1
Utilities for the Simple Game.

P_1 \ P_2	FD	HD
FD	$(0, 0)$	$(2R, 0)$
HD	$(0, 2R)$	(R, R)

(a) High external and self-interference

P_1 \ P_2	FD	HD
FD	$(2R, 2R)$	$(2R, R)$
HD	$(R, 2R)$	(R, R)

(b) Low external interference and perfect SIC

The above game illustrates that FD communications is not always optimal from a network's perspective. To provide a complete characterization of the stable strategy profiles for coexisting FD-enabled links, we account for nodes' SIC capabilities as well as the amount of induced interference from one link on the other in the following Bayesian game.

4 Bayesian Game Between Two Links with Heterogeneous SIC Capabilities

4.1 Game Formulation

The two-player Bayesian game can be defined as $\mathcal{G} = (\mathcal{P}, \mathcal{S}, \Theta, \mathcal{U}, \mathcal{D})$, where $\mathcal{P}$ and $\mathcal{S}$ are as in $\mathcal{G}_s$. The exact expressions for the utility set $\mathcal{U} = \{U_1, U_2\}$ will be defined later. As for Θ and $\mathcal{D}$, they are defined as follows:

Definition 4.1. $\Theta = \{\Theta_1, \Theta_2\}$, where Θ_i is the set of types of P_i.

P_i's type represents its SIC capability, which is characterized by the parameter $\chi_i \in [0, 1]$. χ_i is the ratio between the RSI signal and the transmit power. If $\chi_i = 0$, the corresponding node can completely suppress its self-interference (perfect SIC); otherwise, it can only suppress a fraction $1 - \chi_i$ of its self-interference. For simplicity, we assume that both nodes of P_i have the same χ_i. Although the player's SIC capability (and hence, its type) takes values in the continuous range between 0 and 1, we later show that the NE strategy of P_i will be the same if P_i is of any type between 0 and some threshold χ_i^*. Also, the NE strategy of P_i will be the same if P_i is of any type between χ_i^* and another threshold χ_i^{**}, and it will be the same if P_i is of any type between χ_i^{**} and 1. The two thresholds χ_i^* and χ_i^{**} are derived at the end of this section. Accordingly, we discretize the set of types $\Theta_i \triangleq \{1, 2, 3\}$, and denote the type of player P_i by θ_i, which can take one of three possible values: $\theta_i = 1$ (Type 1) if $\chi_i \in [0, \chi_i^*]$, $\theta_i = 2$ (type 2) if $\chi_i \in [\chi_i^*, \chi_i^{**}]$, and $\theta_i = 3$ (type 3) if $\chi_i \in [\chi_i^{**}, 1]$. Note that θ_1 and θ_2 are independent.

Definition 4.2. $\mathcal{D} = \{D_1, D_2\}$, where D_i is a probability distribution over the types of $P_i, i = 1, 2$.

For $i = 1, 2$, P_i is of type 1 with probability p_{i1}, of type 2 with probability p_{i2}, and of type 3 with probability p_{i3}.

Finally, in Bayesian games, a pure strategy of P_i is a map s_i: $\Theta_i \rightarrow S_i$, prescribing an action for each type of P_i. Strategy spaces, player types, utility functions, and the probability distributions over the types are assumed to be common knowledge to all players. However, a given player knows only its current strategy and type, and does not know the strategies selected by the other player or its true type. In practice, the probability distributions over the types of players can be estimated by collecting statistics about the latest widely implemented SIC techniques in current radio technologies (e.g., Wi-Fi APs, cellular BSs, tablets, etc.).

The motivation for selecting Bayesian games to model this problem is as follows. Although the development of SIC techniques is still in its early stages, it is expected that different radios (e.g., Wi-Fi APs, BSs, TVs, tablets, etc.) will have different SIC capabilities. Achieving perfect SIC may not always be feasible due to imperfections in existing SIC techniques and challenges related to signal reflections, hardware/DSP limitations, etc. Furthermore, assuming that radios know the exact SIC capabilities of neighboring radios is unrealistic. However, knowing the distributions over players' SIC capabilities is more justifiable. Hence, selecting Bayesian games to model this problem, where perfect knowledge about other players' SIC capabilities is unavailable, is well justified.

Next, we analyze the utility U_1 for P_1 (U_2 can be analyzed similarly). First, consider U_1 under the (FD, FD) strategy profile. P_1 benefits from an FD transmission only if no outage/collision occurs at node a or b, i.e., when $\gamma_{ij}^{(\text{FF})} \geq \gamma_{ij}^*, i, j \in \{a, b\}$, where $\gamma_{ij}^{(\text{FF})}$ is the SNR at node j while receiving data from node i under (FD, FD) and γ_{ij}^* is a given reception threshold. Define $\mathbb{1}_{ij}^{(\text{FF})}$ to be an indicator function for a successful transmission from i to j under (FD, FD). $\mathbb{1}_{ij}^{(\text{FF})} = 1$ if $\gamma_{ij}^{(\text{FF})} \geq \gamma_{ij}^*$ and 0 otherwise. Denote the transmission cost from node i by C_i. We set $C_i = c_i P_{t,i}$, where $P_{t,i}$ is the transmission power of node $i, i \in \{a, b, c, d\}$, and c_i is a constant of conversion measured in bits per second per watts. Note that c_i is a design parameter that can be used to reflect the relative importance of the transmission power. The utility of P_1 under (FD, FD), denoted by $U_1^{(\text{FF})}$,

can be expressed as follows:

$$U_1^{(\text{FF})} = \mathbb{1}_{ab}^{(\text{FF})} R_{ab}^{(\text{FF})} + \mathbb{1}_{ba}^{(\text{FF})} R_{ba}^{(\text{FF})} - C_a - C_b \quad (1)$$

where $R_{ab}^{(\text{FF})}$ and $R_{ba}^{(\text{FF})}$ are, respectively, the forward and reverse link throughputs for link (a,b). $R_{ij}^{(\text{FF})}$, $i,j \in \{a,b\}, i \neq j$, is given by:

$$\begin{aligned} R_{ij}^{(\text{FF})} &= \log\left(1+\gamma_{ij}^{(\text{FF})}\right) \\ &= \log\left(1+\frac{P_{t,i}g_{ij}}{\chi_j^2 P_{t,j}g_{jj} + P_{t,c}g_{cj} + P_{t,d}g_{dj} + \sigma_j^2}\right) \end{aligned} \quad (2)$$

where g_{ij} is the channel gain between any two nodes i and $j, i \neq j$, σ_j^2 is the noise power at node j, and g_{jj} is the self-interference channel gain at node j. Note the RSI term in the denominator of the SNR. According to our earlier assumption, $\chi_a = \chi_b \triangleq \chi_1$ (also, $\chi_c = \chi_d \triangleq \chi_2$).

Under (HD, FD) (i.e., P_1 selects HD while P_2 selects FD), P_1's utility, denoted by $U_1^{(\text{HF})}$, includes the throughput of the forward link minus its transmission cost. The same amount of external interference is still induced on P_1, as P_2 still operates in FD mode. Formally, $U_1^{(\text{HF})}$ can be written as:

$$U_1^{(\text{HF})} = \mathbb{1}_{ab}^{(\text{HF})} R_{ab}^{(\text{HF})} - C_a = \mathbb{1}_{ab}^{(\text{HF})} \log\left(1+\gamma_{ab}^{(\text{HF})}\right) - c_a P_{t,a} \quad (3)$$

where $\gamma_{ab}^{(\text{HF})} = P_{t,a}g_{ab} / \left(P_{t,c}g_{cb} + P_{t,d}g_{db} + \sigma_b^2\right)$ is the SNR at b when receiving data from a under (HD, FD).

For the two other strategy profiles, P_1's utility can be written as follows:

$$\begin{aligned} U_1^{(\text{FH})} &= \mathbb{1}_{ab}^{(\text{FH})} \log\left(1+\gamma_{ab}^{(\text{FH})}\right) - c_a P_{t,a} \\ &+ \mathbb{1}_{ba}^{(\text{FH})} \log\left(1+\gamma_{ba}^{(\text{FH})}\right) - c_b P_{t,b} \quad (4) \\ U_1^{(\text{HH})} &= \mathbb{1}_{ab}^{(\text{HH})} \log\left(1+\gamma_{ab}^{(\text{HH})}\right) - c_a P_{t,a} \quad (5) \end{aligned}$$

where $\gamma_{ab}^{(\text{FH})} = P_{t,a}g_{ab} / \left(\chi_b^2 P_{t,b}g_{bb} + P_{t,c}g_{cb} + \sigma_b^2\right)$, $\gamma_{ba}^{(\text{FH})} = P_{t,b}g_{ba} / \left(\chi_a^2 P_{t,a}g_{aa} + P_{t,c}g_{ca} + \sigma_a^2\right)$, and $\gamma_{ab}^{(\text{HH})} = P_{t,a}g_{ab} / \left(P_{t,c}g_{cb} + \sigma_b^2\right)$.

To find the BNE, we first define technical conditions (TCs) under which no outage/collision occurs at the receivers of both players. We start by analyzing the no-outage case to facilitate understanding the Bayesian game analysis. Then, we conclude this section by deriving the BNE for the general case when outage is possible.

Outage will not occur for P_1 iff $\gamma_{ab}^{mn} \geq \gamma_{ab}^*$ and $\gamma_{ba}^{mn} \geq \gamma_{ba}^*, \forall m,n \in S_1$. However, by examining the SNR expressions for different strategy profiles, we notice that the minimum SNR is encountered under (FD, FD) due to the existence of two interference terms from nodes c and d, in addition to the RSI. With the imposed conditions on $\gamma_{ab}^{(\text{FF})}$ and $\gamma_{ba}^{(\text{FF})}$, we can implicitly ensure that no outage occurs under the other strategy profiles. Formally, we define the following two TCs P_1:

$$\text{TC}_{11}\text{:}\ \ P_{t,c}g_{cb} + P_{t,d}g_{db} - \frac{P_{t,a}g_{ab}}{\gamma_{ab}^*} + \chi_1^2 P_{t,b}g_{bb} + \sigma_b^2 < 0 \quad (6)$$

$$\text{TC}_{12}\text{:}\ \ P_{t,c}g_{ca} + P_{t,d}g_{da} - \frac{P_{t,b}g_{ba}}{\gamma_{ba}^*} + \chi_1^2 P_{t,a}g_{aa} + \sigma_a^2 < 0. \quad (7)$$

Two similar TCs can be established for P_2. We later discuss the case when those technical conditions are not satisfied (i.e., an outage may occur).

When χ_i is sufficiently small, P_i can efficiently suppress its self-interference signal, ensuring that the FD strategy dominates the HD strategy. χ_1^* is the value of χ_1 at which $U_1^{(\text{FH})} = U_1^{(\text{HH})}$ and χ_2^* is the value of χ_2 at which $U_2^{(\text{HF})} = U_2^{(\text{HH})}$. As χ_i increases, the higher RSI makes the HD strategy more preferable in some cases (especially if the other player is following the HD strategy). This means that P_1's utility, for example, under (FD, HD) decreases faster with χ_1 than that under (FD, FD). The reason for this is that under (FD, HD), the RSI dominates the external interference (since P_2 is playing HD), which is not the case for the (FD, FD). The same argument applies to player P_2. χ_1^{**} is defined as the value of χ_1 at which $U_1^{(\text{FF})} = U_1^{(\text{HF})}$ and χ_2^{**} is defined as the value of χ_2 at which $U_2^{(\text{FF})} = U_2^{(\text{FH})}$. As χ_i continues to increase beyond χ_i^{**}, the RSI signal will be very high, forcing the utilities under the FD strategy to be lower than that of the HD strategy (irrespective of the other player's strategy). Towards the end of this section, we discuss how χ_i^* and χ_i^{**} can be computed.

4.2 Existence and Uniqueness of a Bayesian NE

Theorem 1. *Game $\mathcal{G}$ has a BNE (s_1^*, s_2^*), which is given by:*

$$s_i^* = \begin{cases} \textit{FD}, & \textit{if } \theta_i = 1 \\ \begin{cases} \textit{FD}, & \textit{if } p_{\hat{i}1} > \alpha_i \\ \textit{FD or HD}, & \textit{if } p_{\hat{i}1} \leq \alpha_i \textit{ and } p_{\hat{i}1} + p_{\hat{i}2} \geq \alpha_i \\ \textit{HD}, & \textit{if } p_{\hat{i}1} + p_{\hat{i}2} < \alpha_i \end{cases}, & \textit{if } \theta_i = 2 \\ \textit{HD}, & \textit{if } \theta_i = 3 \end{cases} \quad (8)$$

for $i \in \{1,2\}$. $\hat{i}$ is the index of node i's peer node (i.e., if $i = 1, \hat{i} = 2$, and vice verse). $\alpha_1, \alpha_2 \in [0,1]$ are defined as:

$$\alpha_1 \overset{def}{=} \frac{U_1^{(HH)} - U_1^{(FH)}}{U_1^{(HH)} - U_1^{(FH)} + U_1^{(FF)} - U_1^{(HF)}} \quad (9)$$

$$\alpha_2 \overset{def}{=} \frac{U_2^{(HH)} - U_2^{(HF)}}{U_2^{(HH)} - U_2^{(HF)} + U_2^{(FF)} - U_2^{(FH)}}. \quad (10)$$

Note that α_i is a function of $\chi_i, i \in \{1,2\}$.

Proof: If player P_1 is of type 1, then $U_1^{(\text{FF})} > U_1^{(\text{HF})}$ and $U_1^{(\text{FH})} > U_1^{(\text{HH})}$, i.e., the FD strategy strictly dominates the HD strategy. On the other hand, if P_1 is of type 3, then $U_1^{(\text{FF})} < U_1^{(\text{HF})}$ and $U_1^{(\text{FH})} < U_1^{(\text{HH})}$, i.e., the HD strategy strictly dominates the FD strategy. Applying the same argument to player P_2, we can determine the BNE if the players are of type 1 or 3, as shown in (8).

The more challenging case occurs when at least one of the players is of type 2. If P_1 is of type 2, then $U_1^{(\text{FF})} > U_1^{(\text{HF})}$ and $U_1^{(\text{FH})} < U_1^{(\text{HH})}$. Therefore, P_1's decision depends on P_2's action. As mentioned earlier, P_2's action will be FD if $\theta_2 = 1$ and HD if $\theta_2 = 3$, however, its action when $\theta_2 = 2$ is not determined yet. First, consider the case when P_2's action is FD and $\theta_2 = 2$. In this case, P_1's FD strategy dominates the HD strategy iff:

$$p_{21}U_1^{(\text{FF})} + p_{22}U_1^{(\text{FF})} + p_{23}U_1^{(\text{FH})} > p_{21}U_1^{(\text{HF})} + p_{22}U_1^{(\text{HF})} + p_{23}U_1^{(\text{HH})}.$$

Second, if P_2's action is HD when $\theta_2 = 2$, then P_1's FD strategy dominates the HD strategy iff:

$$p_{21}U_1^{(\mathrm{FF})} + p_{22}U_1^{(\mathrm{FH})} + p_{23}U_1^{(\mathrm{FH})} > p_{21}U_1^{(\mathrm{HF})} + p_{22}U_1^{(\mathrm{HH})} + p_{23}U_1^{(\mathrm{HH})}.$$

Solving the above two equations along with $p_{21} + p_{22} + p_{23} = 1$, we obtain the value of α_1 and derive the conditions on P_2's probability distribution, as shown in (8). A similar approach is used to determine α_2 for P_2. □

The derived BNE, which represents the stable point for both players, can be interpreted as follows. Since P_i knows its own true type and the probability distribution over the types of the other player, the first step for player P_i is to check its own type. This can be done by calculating its SIC capability, χ_i, by comparing the power of the residual self-interference signal to its original transmission power. If $\chi_i \leq \chi_i^*$, then P_i is of type 1. In this case, P_i plays FD irrespective of what the other player is playing. If $\chi_i \geq \chi_i^{**}$, then P_i is of type 3. In this case, P_i plays HD irrespective of what the other player is playing. Otherwise (i.e., $\chi_i^* < \chi_i < \chi_i^{**}$), player P_i is of type 2. In this case, P_i has to use the probability distribution over the other player types to determine its action by following Theorem 1.

Corollary 1. *If each of the two players P_1 and P_2 satisfies one of the following two conditions:*

$$p_{\hat{i}1} > \alpha_i \quad (11)$$

$$p_{\hat{i}1} + p_{\hat{i}2} < \alpha_i \quad (12)$$

where $i \in \{1, 2\}$ and $\hat{i}$ is the index of node i's peer node, then game $\mathcal{G}$ has a unique BNE, which is given by:

$$((F,F,H),(F,F,H)) \quad \textit{if} \quad p_{21} > \alpha_1 \;\&\; p_{11} > \alpha_2 \quad (13)$$

$$((F,F,H),(F,H,H)) \quad \textit{if} \quad p_{21} > \alpha_1 \;\&\; p_{11} + p_{12} < \alpha_2 \quad (14)$$

$$((F,H,H),(F,F,H)) \quad \textit{if} \quad p_{21} + p_{22} < \alpha_1 \;\&\; p_{11} > \alpha_2 \quad (15)$$

$$((F,H,H),(F,H,H)) \quad \textit{if} \quad p_{21} + p_{22} < \alpha_1 \;\&\; p_{11} + p_{12} < \alpha_2 \quad (16)$$

where the notation $((F,F,H),(F,H,H))$, for instance, means that P_1 operates in the FD mode when $\theta_1 = 1$ or 2 and in the HD mode when $\theta_1 = 3$, while P_2 operates in the FD mode when $\theta_2 = 1$ and in the HD mode when $\theta_2 = 2$ or 3.

Proof: The two-player Bayesian game $\mathcal{G}$ (with each player having one of three possible types) can be equivalently formulated as a 2^3-by-2^3 strategic game. From Theorem 1 and its proof, it can be shown that under each of the conditions stated in (13)-(16), the corresponding strategy profile consists of a strictly dominating strategy for each player in the 8-by-8 game. Hence, the BNE is unique. □

Corollary 2. *If exactly one of the players satisfies neither* (11) *nor* (12)*, then game $\mathcal{G}$ has two BNEs (from the strategy profiles given by* (13)-(16)*).*

Proof: Based on Theorem 1, player P_i always plays FD if $\theta_i = 1$ and always plays HD if $\theta_i = 3$. If $\theta_i = 2$, then the BNE is decided based on the relation between $p_{\hat{i}1}$, $p_{\hat{i}2}$, and α_i. Specifically, if (11) or (12) is satisfied, then player P_i plays FD or HD, respectively. However, if neither conditions are satisfied, then playing FD or HD is equivalent (see proof of Theorem 1).

While Corollary 1 illustrates the case where each of the two players P_1 and P_2 satisfies one of the two conditions shown in (11) and (12), Corollary 2 focuses on the scenario where *exactly* one of the players neither satisfies (11) nor (12). Under this scenario, one player can either play HD or FD (both are equivalent), while the other player has to play only a single strategy (either HD or FD based on Theorem 1 rules). Hence, two of the four BNEs defined in Corollary 1 will be valid simultaneously under Corollary 2. As an example, if we assume that only P_1 satisfies neither (11) nor (12), then the two BNEs will be ((F, F, H), (F, F, H)) and ((F, F, H), (F, H, H)) if $p_{21} > \alpha_1$. On the other hand, if $p_{21} + p_{22} < \alpha_1$, then the two BNEs will be ((F, H, H), (F, F, H)) and ((F, H, H), (F, H, H)). □

Corollary 3. *If both players satisfy neither* (11) *nor* (12)*, then the game has the four BNEs, given by* (13)-(16)*.*

Proof: The proof of Corollary 3 is very similar to that of Corollary 2 (it follows directly from Theorem 1 and Corollary 1). When both players satisfy neither (11) nor (12), then both players can either play FD or HD. Hence, the game has the four BNEs, given by (13)-(16). □

4.3 Accounting for Link Outages

We now relax the technical conditions ((6) and (7) for P_1 and two similar conditions for P_2), and assume that any of the forward/reverse links may experience outage. In this case, the relation between χ_i^* and χ_i^{**} is not fixed (i.e., χ_i^* could be larger or smaller than χ_i^{**}). The reason is that in the case of outage, if P_2 operates in the FD mode, then $U_1^{(\mathrm{FF})}$ may decrease faster with χ_1 compared to $U_1^{(\mathrm{FH})}$, and hence as χ_1 increases the condition $U_1^{(\mathrm{FF})} = U_1^{(\mathrm{HF})}$ may be satisfied before the condition $U_1^{(\mathrm{FH})} = U_1^{(\mathrm{HH})}$. Therefore, $\chi_1^{**} < \chi_1^*$ (recall the definition of χ_1^* and χ_1^{**} in Section 4.1). The same situation arises in the case of P_2 under the possibility of outage.

Theorem 2. *Theorem 1 and Corollaries 1-3 hold true for game $\mathcal{G}$ under the possibility of outage. However, $\theta_i, i \in \{1, 2\}$, in this case, is given by:*

$$\theta_i = \begin{cases} 1, & \textit{if } \chi_i \leq \min(\chi_i^*, \chi_i^{**}) \\ 2, & \textit{if } \min(\chi_i^*, \chi_i^{**}) < \chi_i < \max(\chi_i^*, \chi_i^{**}) \\ 3, & \textit{if } \chi_i \geq \max(\chi_i^*, \chi_i^{**}). \end{cases} \quad (17)$$

Proof: From the definitions of χ_i^* and χ_i^{**} in Section 4.1, it can be shown that irrespective whether outage occurs or not, the dominating strategy of player P_i when $\chi_i \leq \min(\chi_i^*, \chi_i^{**})$ is FD, and when $\chi_i \geq \max(\chi_i^*, \chi_i^{**})$ is HD. When $\min(\chi_i^*, \chi_i^{**}) < \chi_i < \max(\chi_i^*, \chi_i^{**})$, following the same approach in the proof of Theorem 1 (by deriving the conditions under which P_i's expected utility under the FD strategy is higher than that under the HD strategy while fixing the other player strategy, and solving the two resulting inequalities along with $p_{21} + p_{22} + p_{23} = 1$), it can be shown that the dominating strategy is given by (8) when $\theta_i = 2$. Hence, Theorem 2 holds. □

Next, we derive closed-form expressions for χ_1^* and χ_1^{**}. In this derivation, we focus on player P_1; a similar approach

could be used to derive the thresholds of player P_2. The challenge in this derivation is the presence of the indicator functions along with the logarithmic terms.

We start by deriving χ_1^{**}, which occurs when $U_1^{(\text{FF})} = U_1^{(\text{HF})}$. Substituting in the previous equation using (1) and (3), we get the following:

$$\mathbb{1}_{ab}^{(\text{FF})} R_{ab}^{(\text{FF})} + \mathbb{1}_{ba}^{(\text{FF})} R_{ba}^{(\text{FF})} - C_a - C_b = \mathbb{1}_{ab}^{(\text{HF})} R_{ab}^{(\text{HF})} - C_a. \quad (18)$$

Rearranging the above equation, we get $\mathbb{1}_{ab}^{(\text{FF})} R_{ab}^{(\text{FF})} + \mathbb{1}_{ba}^{(\text{FF})} R_{ba}^{(\text{FF})} = w$, where $w \stackrel{\text{def}}{=} \mathbb{1}_{ab}^{(\text{HF})} R_{ab}^{(\text{HF})} + C_b$ is a term that does not depend on χ_1.

In the following analysis, we assume that the link throughput is measured in nats per second (i.e., using the natural logarithm). Substituting the expressions for $R_{ab}^{(\text{FF})}$ and $R_{ba}^{(\text{FF})}$ in (2), we get the following:

$$\begin{aligned} w &= \mathbb{1}_{ab}^{(\text{FF})} R_{ab}^{(\text{FF})} + \mathbb{1}_{ba}^{(\text{FF})} R_{ba}^{(\text{FF})} \\ &= \mathbb{1}_{ab}^{(\text{FF})} \ln\left(1 + \frac{P_{t,a} g_{ab}}{\chi_1^{**2} P_{t,b} g_{bb} + P_{t,c} g_{cb} + P_{t,d} g_{db} + \sigma_b^2}\right) \\ &+ \mathbb{1}_{ba}^{(\text{FF})} \ln\left(1 + \frac{P_{t,b} g_{ba}}{\chi_1^{**2} P_{t,a} g_{aa} + P_{t,c} g_{ca} + P_{t,d} g_{da} + \sigma_a^2}\right) \\ &= \ln\left(1 + \frac{P_{t,a} g_{ab}}{\chi_1^{**2} P_{t,b} g_{bb} + P_{t,c} g_{cb} + P_{t,d} g_{db} + \sigma_b^2}\right)^{\mathbb{1}_{ab}^{(\text{FF})}} \\ &+ \ln\left(1 + \frac{P_{t,b} g_{ba}}{\chi_1^{**2} P_{t,a} g_{aa} + P_{t,c} g_{ca} + P_{t,d} g_{da} + \sigma_a^2}\right)^{\mathbb{1}_{ba}^{(\text{FF})}} \end{aligned}$$

$$w = \ln\left[\left(1 + \frac{P_{t,a} g_{ab}}{\chi_1^{**2} P_{t,b} g_{bb} + u}\right)^{\mathbb{1}_{ab}^{(\text{FF})}} \left(1 + \frac{P_{t,b} g_{ba}}{\chi_1^{**2} P_{t,a} g_{aa} + v}\right)^{\mathbb{1}_{ba}^{(\text{FF})}}\right] \quad (19)$$

where $u \stackrel{\text{def}}{=} P_{t,c} g_{cb} + P_{t,d} g_{db} + \sigma_b^2$ and $v \stackrel{\text{def}}{=} P_{t,c} g_{ca} + P_{t,d} g_{da} + \sigma_a^2$ are independent of χ_1.

To obtain an expression for χ_1^{**}, we need to consider different combinations of the values of the indicator functions $\mathbb{1}_{ab}^{(\text{FF})}$ and $\mathbb{1}_{ba}^{(\text{FF})}$ (four cases). For the first case ($\mathbb{1}_{ab}^{(\text{FF})} = \mathbb{1}_{ba}^{(\text{FF})} = 0$), an outage will occur at both receivers of player P_1. In this case, P_1's utility under the FD strategy cannot be higher than his utility under the HD strategy. Hence, $\chi_{11}^{**} = 0$, where χ_{ij}^{**} is defined as the value of χ_i^{**} under case j.

The second case occurs when $\mathbb{1}_{ab}^{(\text{FF})} = 0$ and $\mathbb{1}_{ba}^{(\text{FF})} = 1$. Substituting with those values in (19) and after some manipulations, we get the following expression:

$$P_{t,b} g_{ba} = (e^w - 1)\left(\chi_{12}^{**2} P_{t,a} g_{aa} + v\right). \quad (20)$$

Therefore, under case 2, χ_{12}^{**} can be expressed as follows:

$$\chi_{12}^{**} = \sqrt{\left(\frac{1}{P_{t,a} g_{aa}}\right)\left(\frac{P_{t,b} g_{ba}}{e^w - 1} - v\right)}. \quad (21)$$

Similarly, for case 3, where $\mathbb{1}_{ab}^{(\text{FF})} = 1$ and $\mathbb{1}_{ba}^{(\text{FF})} = 0$, χ_{13}^{**} can be expressed as follows:

$$\chi_{13}^{**} = \sqrt{\left(\frac{1}{P_{t,b} g_{bb}}\right)\left(\frac{P_{t,a} g_{ab}}{e^w - 1} - u\right)}. \quad (22)$$

Finally, under case 4 (i.e., $\mathbb{1}_{ab}^{(\text{FF})} = 1$ and $\mathbb{1}_{ba}^{(\text{FF})} = 1$), we substitute the values of the indicator functions in (19) and get the following equation:

$$\beta_1 \chi_{14}^{**4} + \beta_2 \chi_{14}^{**2} + \beta_3 = 0. \quad (23)$$

where $\beta_1 = P_{t,a} P_{t,b} g_{aa} g_{bb} (1 - e^w)$, $\beta_2 = (P_{t,b} g_{bb} v + P_{t,a} g_{aa} u)(1 - e^w) + P_{t,b}^2 g_{ba} g_{bb} + P_{t,a}^2 g_{ab} g_{aa}$, and $\beta_3 = uv(1 - e^w) + P_{t,b} g_{ba} u + P_{t,a} g_{ab} v + P_{t,a} P_{t,b} g_{ab} g_{ba}$. Equation (23) can be solved easily using the quadratic formula. To sum up the four cases, the value of χ_1^{**} can be expressed as follows:

$$\chi_1^{**} = \begin{cases} 0, & \text{if } \mathbb{1}_{ab}^{(\text{FF})} = \mathbb{1}_{ba}^{(\text{FF})} = 0 \\ \sqrt{\left(\frac{1}{P_{t,a} g_{aa}}\right)\left(\frac{P_{t,b} g_{ba}}{e^w - 1} - v\right)}, & \text{if } \mathbb{1}_{ab}^{(\text{FF})} = 0,\ \mathbb{1}_{ba}^{(\text{FF})} = 1 \\ \sqrt{\left(\frac{1}{P_{t,b} g_{bb}}\right)\left(\frac{P_{t,a} g_{ab}}{e^w - 1} - u\right)}, & \text{if } \mathbb{1}_{ab}^{(\text{FF})} = 1,\ \mathbb{1}_{ba}^{(\text{FF})} = 0 \\ \sqrt{\frac{-\beta_2 - \sqrt{\beta_2^2 - 4\beta_1\beta_3}}{2\beta_1}}, & \text{if } \mathbb{1}_{ab}^{(\text{FF})} = \mathbb{1}_{ba}^{(\text{FF})} = 1 \end{cases} \quad (24)$$

The above approach can also be used to derive χ_1^*, resulting in:

$$\chi_1^* = \begin{cases} 0, & \text{if } \mathbb{1}_{ab}^{(\text{FH})} = \mathbb{1}_{ba}^{(\text{FH})} = 0 \\ \sqrt{\left(\frac{1}{P_{t,a} g_{aa}}\right)\left(\frac{P_{t,b} g_{ba}}{e^{\hat{w}} - 1} - \hat{v}\right)}, & \text{if } \mathbb{1}_{ab}^{(\text{FH})} = 0,\ \mathbb{1}_{ba}^{(\text{FH})} = 1 \\ \sqrt{\left(\frac{1}{P_{t,b} g_{bb}}\right)\left(\frac{P_{t,a} g_{ab}}{e^{\hat{w}} - 1} - \hat{u}\right)}, & \text{if } \mathbb{1}_{ab}^{(\text{FH})} = 1,\ \mathbb{1}_{ba}^{(\text{FH})} = 0 \\ \sqrt{\frac{-\hat{\beta}_2 - \sqrt{\hat{\beta}_2^2 - 4\hat{\beta}_1\hat{\beta}_3}}{2\hat{\beta}_1}}, & \text{if } \mathbb{1}_{ab}^{(\text{FH})} = \mathbb{1}_{ba}^{(\text{FH})} = 1 \end{cases} \quad (25)$$

where $\hat{w} \stackrel{\text{def}}{=} \mathbb{1}_{ab}^{(\text{HH})} R_{ab}^{(\text{HH})} + C_b$, $\hat{u} \stackrel{\text{def}}{=} P_{t,c} g_{cb} + \sigma_b^2$ and $\hat{v} \stackrel{\text{def}}{=} P_{t,c} g_{ca} + \sigma_a^2$, $\hat{\beta}_1 = P_{t,a} P_{t,b} g_{aa} g_{bb} (1 - e^{\hat{w}})$, $\hat{\beta}_2 = (P_{t,b} g_{bb} \hat{v} + P_{t,a} g_{aa} \hat{u})(1 - e^{\hat{w}}) + P_{t,b}^2 g_{ba} g_{bb} + P_{t,a}^2 g_{ab} g_{aa}$, and $\hat{\beta}_3 = \hat{u}\hat{v}(1 - e^{\hat{w}}) + P_{t,b} g_{ba} \hat{u} + P_{t,a} g_{ab} \hat{v} + P_{t,a} P_{t,b} g_{ab} g_{ba}$.

5 Extension to Multiple Links with Heterogeneous SIC Capabilities

In Section 4, we studied the coexistence problem between two links with heterogeneous SIC capabilities in a Bayesian game-theoretic framework. In this section, we extend the treatment to more than two links.

5.1 Approximation of the Network Interference Graph

Due to the complexity of deriving the BNE of a game that involves more than two links, we simplify the interactions (i.e., interference relations) between the multiple FD-enabled links. Specifically, we approximate the network interference graph, as depicted in Figure 2. In the exact interference graph, shown in Figure 2(a), each link is affected by all other links in the network. Instead, in the proposed approximation, we assume that each link is only affected by a single link in the network, which is its dominant interfering link[1]. We consider a distance-dependent interference (i.e., path-loss), where the dominant interfering link of, say link 1, will be the closest link. Because links are FD-enabled, both nodes of a link are transceivers, and we compute the distance between two links as the distance between the midpoints of the segments that connect the two transceivers of each link.

1. This assumption has been used in the wireless communications and networking literature [36, 37].

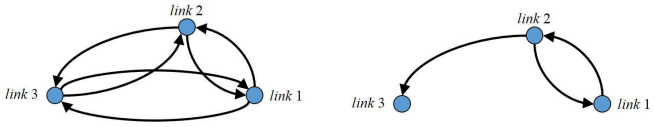

(a) Exact (b) Approximate

Fig. 2. Approximation of the network interference graph.

5.2 FD/HD Mode Selection

In this section, we first derive the structure of the network interference graph under the aforementioned approximation. Then, we discuss our FD/HD mode selection game.

Proposition 1. *The approximate network interference graph consists of loops, each comprised of two links only, with branches attached to them, as shown in Figure 3. Note that an interference graph, in general, have multiple loops. The figure shows only one of them.*

Proof: To derive the structure of the approximate interference graph, let us start with one FD-enabled link, say link 1 in Figure 4(a), and its dominant interfering link, say link 2. Then, the dominant interfering link of link 2 can be one of the following:

- Link 1, in which case, links 1 and 2 will be engaged in a two-player game, or
- Another link, say link 3 in Figure 4(a), in which case, the distance between links 2 and 3, denoted by d_{23}, needs to be smaller than the distance between links 1 and 2 (d_{12}). At the same time, d_{13} needs to be larger than d_{12} (because link 2 is the dominant interfering link of link 1). Hence, $d_{13} > d_{12} > d_{23}$.

Now, if we assume that there are only three links in the network, then link 2 is also the dominant interfering link of link 3, and links 2 and 3 will be engaged in a two-player game. The interference graph in this case is shown in Figure 4(a). On the other hand, if we assume that there is another link, say link 4, that is closer to link 3 than link 2 (i.e., $d_{34} < d_{23}$), as shown in Figure 4(b), then, $d_{34} < d_{23} < d_{24}$, where the last inequality is because link 3 is the dominant interfering link of link 2. Furthermore, $d_{34} < d_{23} < d_{12} < d_{14}$, where the last two inequalities are because link 3 is the dominant interfering link of link 2 and link 2 is the dominant interfering link of link 1, respectively. Since d_{34} is smaller than both d_{24} and d_{14}, link 3 is also the dominant interfering link of link 4, and links 3 and 4 will be engaged in a two-player game. The interference graph in this case is shown in Figure 4(b).

From the above discussion, we can see that the approximate interference graph consists of loops, each of two links only, with branches attached to them, as shown in Figure 3. □

Based on the above, the unique BNE of the multi-player game can be obtained by applying Algorithm 1.

6 Performance Evaluation

In this section, we conduct numerical evaluations and LabVIEW/MATLAB simulations to assess the performance of our proposed game-theoretic analysis.

Algorithm 1 Finding the unique BNE of the multi-player game

Identify all loops in the network.

Solve their corresponding two-player Bayesian games (i.e., compute the BNE), as in Section 4.

for each loop **do**

  if there is a link attached to this loop (e.g., links 3 and 4 in Figure 3) **then**
    Compute its best-response strategy to the derived BNE in Step (1).
  end if

  if there is a link that is two-hop away from the loop (e.g., link 5 in Figure 3) **then**
    Compute its best-response strategy to the best-response strategy computed in the previous step.
  end if

  Continue in the same way until reaching the leafs of the interference graph.
end for

6.1 Numerical Results

In this section, we evaluate via numerical analysis the characteristics and structure of the BNE for the two-player game. Unless stated otherwise, we use the following parameter values: The channel gain between nodes i and j, g_{ij}, is set to $1, \forall i, j \in \{a, b, c, d\}$, $\sigma_i^2 = 1$ Watt, and the normalized transmission cost c_i is set 0.001.

Figure 5 depicts the expected utility for P_1 vs. χ_1 at different values of *interference channel gains* (ICGs) (i.e., channel gains between the transmitters of P_1 and the receivers of P_2, and vice versa). As shown in the figure, increasing the ICGs reduces the expected utility of P_1. If P_1 is of type 1, its expected utility decreases with χ_1, as P_1 operates in the FD mode, whereas when it is of type 3, its expected utility is constant because it operates in the HD mode. When P_1 is of type 2, P_1 starts operating in the FD mode as χ_1 increases (since $p_{21} > \alpha_1$), and eventually it switches to the HD mode when α_1 exceeds p_{21}. The expected utility when $\theta_1 = 2$ first decreases with χ_1 and then remains constant. Note that the SIC thresholds are different for different ICGs (we only show these thresholds when ICG$= 0.01$). In Figure 6, we show P_1's expected utility for different values of p_{21} (a priori probability that P_2 is of type 1). As p_{21} increases, P_1's expected utility decreases. The reason is that if p_{21} is sufficiently small (e.g., $p_{21} = 0.1$), the expected interference level is relatively low and hence higher expected utility can be achieved.

Figure 7 shows the SIC thresholds of P_1 and P_2 vs. $P_{t,c}$. Under conditions (6) and (7) for P_1 and the two similar conditions for P_2, $\chi_i^* < \chi_i^{**} \forall i$. Because $P_{t,c}$ is the dominating term in $\gamma_{ab}^{(\mathrm{HH})}$, increasing $P_{t,c}$ causes $U_1^{(\mathrm{HH})}$ to decrease faster than $U_1^{(\mathrm{FH})}$. Hence, χ_1^* increases with $P_{t,c}$. A similar argument can be made regarding χ_1^{**}. On the other hand, increasing $P_{t,c}$ causes $U_2^{(\mathrm{HF})}$ to decrease faster than $U_2^{(\mathrm{HH})}$. Hence, χ_2^* decreases with $P_{t,c}$. In Figure 8, we plot the players' expected utilities vs. p_{21} for different values of p_{11}. As p_{21} increases, P_1's expected utility decreases.

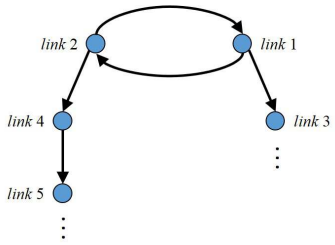

Fig. 3. Generalized approximate network interference graph.

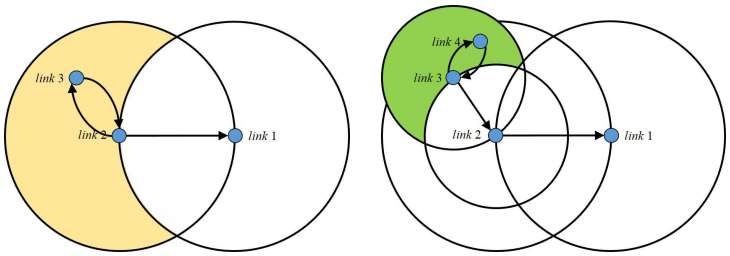

(a) Three FD-enabled links (b) Four FD-enabled links

Fig. 4. Approximate network interference graph for three and four FD-enabled links.

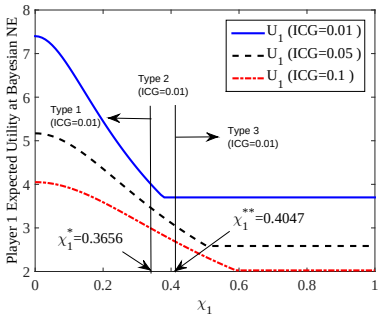

Fig. 5. P_1's expected utility at BNE vs. χ_1 ($\chi_2 = 0$, uniform distribution over the types of both players, and $P_{t,i} = 100$ Watts $\forall i$).

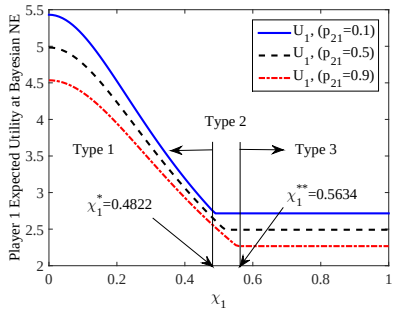

Fig. 6. P_1's expected utility at BNE vs. χ_1 ($\chi_2 = 0$, uniform distribution over P_1 types, $p_{22} = p_{23} = (1 - p_{21})/2$, ICGs$= 0.05$, and $P_{t,i} = 100$ Watts $\forall i$).

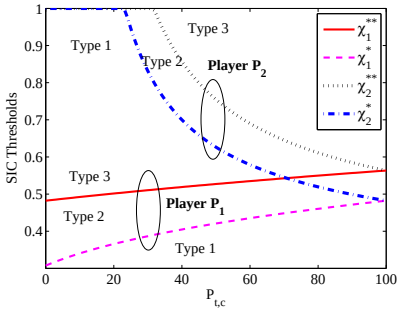

Fig. 7. SIC thresholds for P_1 and P_2 vs. $P_{t,c}$ (ICGs$= 0.05$ and $P_{t,i} = 100$ Watts $\forall i$).

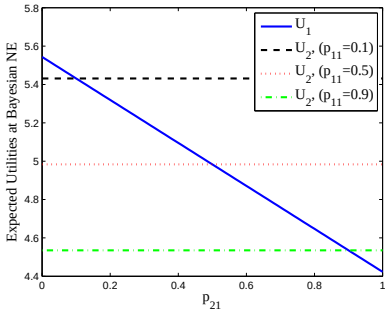

Fig. 8. Expected utilities of P_1 and P_2 at BNE vs. p_{21} ($\chi_1 = \chi_2 = 0$, ICGs$= 0.05$, and maximum transmission powers).

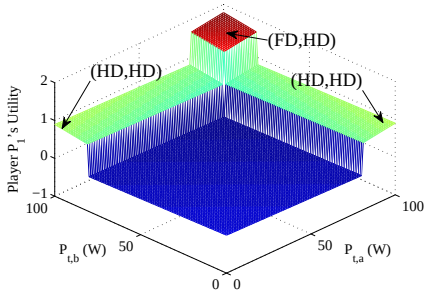

Fig. 9. Player P_1's utility vs. its transmission powers, $P_{t,a}$ and $P_{t,b}$ ($\chi_1 = 0$, P_2 operates in the HD mode, and $P_{t,c} = 100$ Watts).

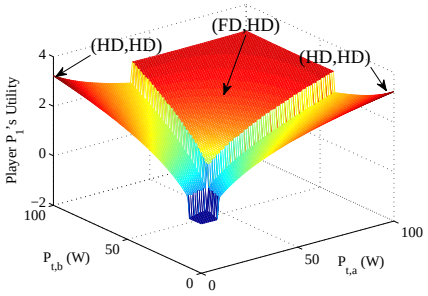

Fig. 10. Player P_1's utility vs. its transmission powers, $P_{t,a}$ and $P_{t,b}$ ($\chi_1 = 0.4$, P_2 operates in the HD mode, and $P_{t,c} = 100$ Watts).

Similarly, P_2's expected utility decreases with p_{11}, whereas it is constant with p_{21}, because P_2 already knows its type.

In the next two figures, we consider the case where an outage may occur at the receiver of any player. Even with complete SIC, when both players operate in the FD mode, outage may occur at all receivers, resulting in negative utilities for both players (because of the transmission costs). However, when P_2 operates in the HD mode, P_1 starts getting a positive utility, as shown in Figure 9. Note that P_1 doubles its throughput in the (FD, HD) strategy profile compared to (HD, HD) when the maximum transmission power is used. However, as P_1's transmission power decreases, outage occurs. Figure 10 shows the case when $\chi_1 = 0.4$. In this case, P_1's utility under (HD, HD) with $P_{t,c} = 10$ Watts is higher than that under (FD, HD). This is due to the increase in RSI level. Figure 11 shows the variation of P_1's expected utility at BNE vs. constant c, which is used to model the transmission power cost, at different SIC values and different ICGs. As c increases, player 1 expected utility decreases linearly as more weight is given to the transmission power cost. Increasing χ_1 and the ICGs decreases P_1's expected utility due to the increase in the residual self-interference and the external interference, respectively.

6.2 Simulations

6.2.1 *Two Links*

In this section, we study via LabVIEW simulations the BER of different players assuming two links only. LabVIEW 2014 software, developed by National Instruments, is used to acquire, analyze, and visualize data. The simulation setup is as follows. We consider a single-channel FD network consisting of two links with different SIC capabilities. Each link can operate in the HD or FD modes. For transmission,

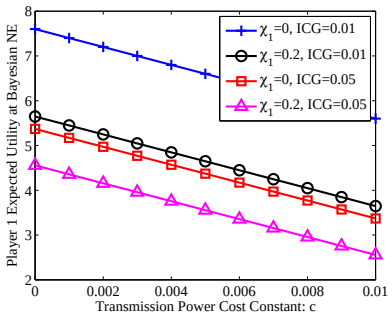

Fig. 11. P_1's expected utility at BNE vs. c ($\chi_2 = 0$, uniform distribution over the types of both players, and $P_{t,i} = 100$ Watts $\forall i$).

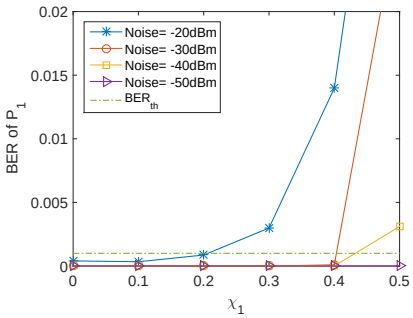

Fig. 12. P_1's forward-link BER vs. χ_1 at different noise levels (no external interference, simulations).

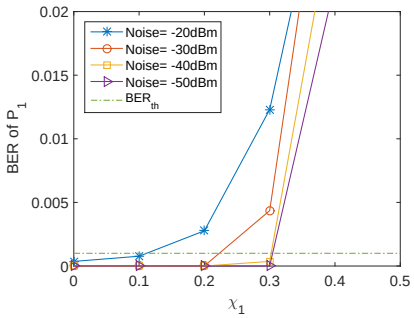

Fig. 13. Forward-link BER of P_1 vs. χ_1 at different noise levels. P_2 operates in the FD mode (ICGs $= 0.01$, simulations).

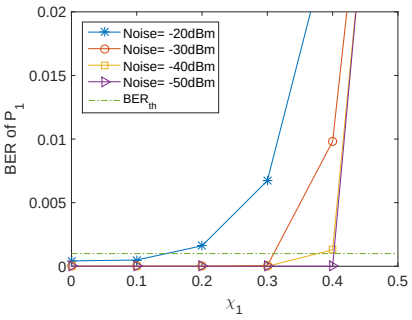

Fig. 14. Forward-link BER of P_1 vs. χ_1 at different noise levels. P_2 operates in the HD mode (ICG $= 0.01$, simulations).

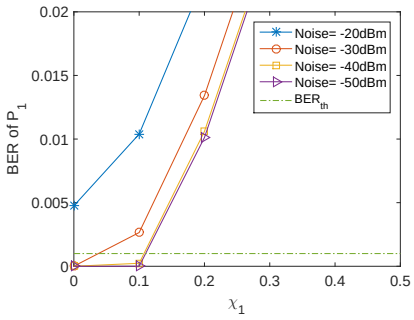

Fig. 15. Forward-link BER of P_1 vs. χ_1 at different noise levels. P_2 operates in the FD mode (ICGs $= 0.04$, simulations).

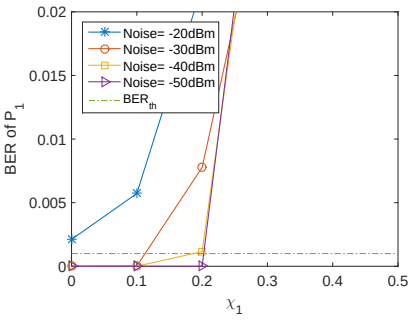

Fig. 16. Forward-link BER of P_1 vs. χ_1 at different noise levels. P_2 operates in the HD mode (ICGs $= 0.09$, simulations).

we generate back-to-back packets, each consisting of 500 bits, modulated using QPSK and $1/2$ code rate. We then add control information (e.g., training sequence) and pass them to the pulse shaping block for transmission. The simulation parameters include the mean of the Gaussian noise (varied from -20 dBm to -50 dBm), ICGs $= \{0.01, 0.04, 0.09\}$, and SIC capabilities (between 0 and 0.5). We focus on the more practical case where χ_i is low. Both the players' channel coefficient and the self-interference channel coefficient are fixed at $0.707 + 0.707i$ (gain $= 1$). For each simulation run, we take the average of 1000 iterations (i.e., 1000 back-to-back packets). We fix the channel phase at $\pi/4$ and set the BER threshold needed for correct reception to $\text{BER}_{\text{th}} = 10^{-4}$.

Figure 12 shows the BER for the forward-link of P_1 vs. χ_1 at different noise levels when P_2 is not transmitting. Depending on the noise level and the SIC capability, P_1 decides to operate in the HD or FD modes. This figure shows the effect of RSI (due to incomplete SIC) on the BER of P_1. As expected, the BER of P_1 increases with χ_1. Specifically, P_1 operates in the FD mode for all values of χ_1 at which the average BER is below BER_{th}. Once the average BER exceeds BER_{th} (i.e., the receiver is not able to decode the packet), the optimal communication mode for P_1 becomes HD. As shown in Figure 12, the threshold value of χ_1 for switching from FD to HD decreases with the noise level; when the noise level is -50 dBm, this threshold equals 1 (i.e., P_1 always operates in the FD mode), whereas when the noise equals -20 dBm, this threshold equals 0.2 (i.e., P_1 operates in the FD mode if $\chi_1 < 0.2$ and operates in the HD mode otherwise).

Figures 13 and 14 show the forward-link BER of P_1 vs. χ_1 at different noise levels, when P_2 operates in the FD and HD modes, respectively. For both figures, the channel coefficients are $0.0707 + 0.0707i$ (ICGs $= 0.01$). As expected, the threshold values of χ_1 under the (FD, FD) strategy profile are lower than those under (FD, HD) for the same noise levels. This means that the range of SIC capabilities for P_1 to operate in the FD mode is narrower when P_2 operates in the FD mode compared to the case when P_2 operates in the HD mode. The reason is that when P_2 operates in the FD mode, it induces higher interference on P_1 than when it operates in the HD mode, which causes outage to occur sooner at P_1 (i.e., at smaller values of χ_1). Comparing Figure 12 to Figures 13 and 14, the range of χ_1 under which P_1 operates in the FD mode is higher when P_2 is off compared to the case when it is transmitting. We repeat the above setup for different ICG values. We present samples of the results in Figures 15 and 16. Figure 15 shows the forward-link BER of P_1 vs. χ_1 at different noise levels, when P_2 operates in the FD mode. In this figure, the channel coefficients are $0.1414 + 0.1414i$ (ICG $= 0.04$). Figure 16 shows the forward-link BER of P_1 vs. χ_1 at different noise levels, when P_2 operates in the HD mode and the ICG $= 0.09$. Similar conclusions can be made regarding the regions of the FD and HD modes for P_1 as the ICGs increase and as P_2 changes its mode from HD to FD.

6.2.2 *More Than Two Links*

In this section, we evaluate the network utility under the BNE, considering a network with more than two FD-enabled links in the network. The simulation setup is as follows. We consider a square area of 200×200 square

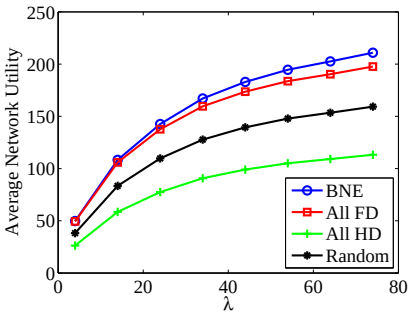

Fig. 17. Average network utility vs. λ (perfect SIC).

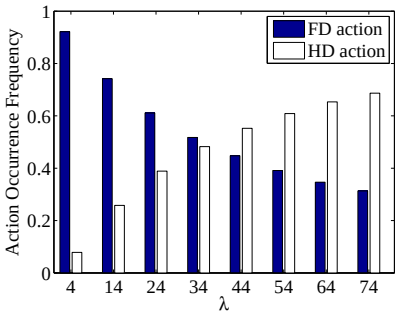

Fig. 18. Histogram of link actions under BNE vs. λ (perfect SIC).

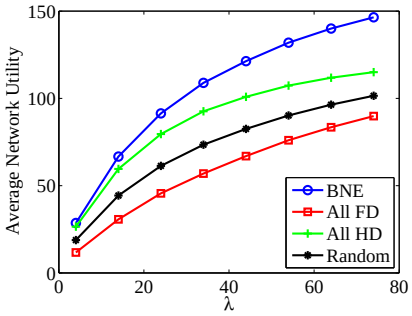

Fig. 19. Average network utility vs. λ $(\chi_{\max} = 2 \times 10^{-4})$.

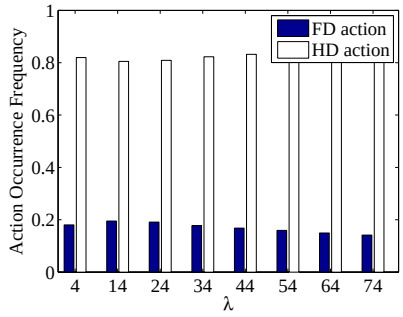

Fig. 20. Histogram of link actions under BNE vs. λ $(\chi_{\max} = 2 \times 10^{-4})$.

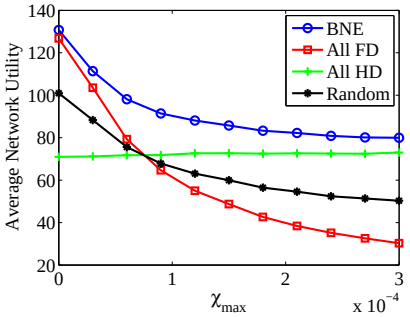

Fig. 21. Average network utility vs. $\chi_{\max}$ $(\lambda = 20)$.

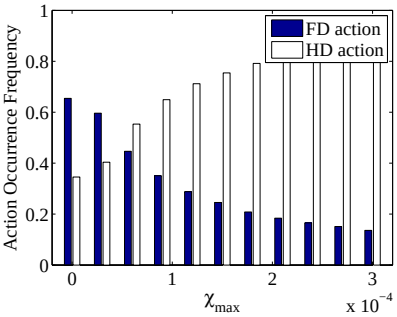

Fig. 22. Histogram of link actions under BNE vs. $\chi_{\max}$ $(\lambda = 20)$.

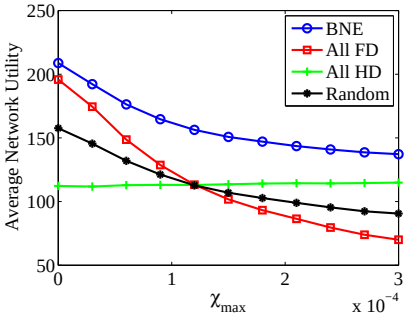

Fig. 23. Average network utility vs. $\chi_{\max}$ $(\lambda = 70)$.

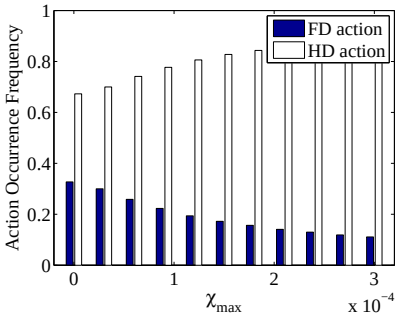

Fig. 24. Histogram of link actions under BNE vs. $\chi_{\max}$ $(\lambda = 70)$.

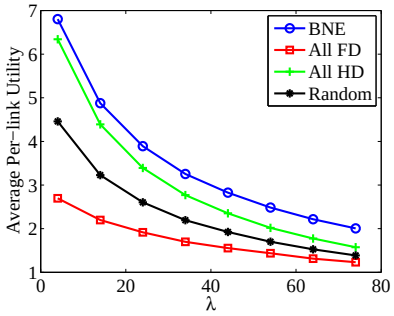

Fig. 25. Average per-link utility vs. λ $(\chi_{\max} = 2 \times 10^{-4})$.

meters, which contains multiple players (i.e., links) that are distributed according to a Poisson point process (PPP). Specifically, we randomly distribute the links' receivers in the specified area according to the PPP with parameter λ ($\lambda \in [4, 80]$). For each receiver, we assign a single transmitter whose location is uniformly distributed in a square of side length 20 meters around the corresponding receiver. We model the players' SIC capability (χ) as an uniformly distributed random variable in $[0, \chi_{\max}]$ ($\chi_{\max}$ is a controllable parameter). An example of this multi-link wireless network could be a residential area with multiple Wi-Fi APs that communicate with Wi-Fi stations (STAs) and coexist with multiple LTE-U small cells base stations in the 5 GHz band.

We model the wireless channels between nodes using the free-space path loss model. The transmission power is 20 dBm, receiver noise power is -90 dBm, antenna gain is 1, carrier frequency is 5 GHz, and the path-loss exponent is 3.5. In the following simulation results and according to the discussion in Section 5, we first determine the loops in the network, where every two players belonging to a loop play the two-player Bayesian game discussed in Section 4 and take the corresponding action (i.e., play according to the derived BNE). In the second step, players that do not belong to any loop play their best-response strategy according to the received interference from their dominant link and the value of their own SIC capabilities. In our simulations, we compare players' sum utilities under the BNE with three basic schemes. *'All FD'* and *'All HD'* schemes correspond to *'all'* players in the network playing FD and HD, respectively. The third scheme is called *random* in which all players select the FD action with probability 0.5.

Figure 17 shows average network utility versus λ at perfect SIC for the four schemes under consideration (BNE, All FD, All HD, and random). Although all players have perfect SIC, playing FD all the time (i.e., 'All FD') is not the optimal scheme since external interference between players

can be significant. Note that according to our earlier discussion in Section 4, the derived BNE is the equilibrium and optimal strategy profile. As expected, the sum utilities under the random scheme is between the 'All HD' and 'All FD' utilities. Figure 18 shows the normalized histogram of various actions versus λ under the BNE with perfect SIC. At low λ values, the FD action dominates the HD action since the amount of external interference is small. As λ increases (i.e., network becomes more dense), the FD action occurs less often, while the HD action occurs more often. Figure 19 shows the average network utility versus λ at $\chi_{\max} = 2 \times 10^{-4}$ for the four schemes. In contrast to the perfect SIC case, in Figure 19, the 'All HD' scheme outperforms the 'All FD' scheme, while the BNE returns the maximum utility for the whole network. Figure 20 shows the normalized histogram of various actions versus λ under the BNE at $\chi_{\max} = 2 \times 10^{-4}$. Similar to Figure 18, as λ increases, the FD action occurs less often than the HD action. Note that the occurrence frequencies of the modes is varying very slowly with λ since the HD mode is dominating the FD mode due to low SIC capabilities.

In the next set of simulations, we vary $\chi_{\max}$ in the interval $[0, 3 \times 10^{-4}]$ and compare the average network utility under the four schemes for different values of λ. Figure 21 shows the average network utility versus $\chi_{\max}$ at $\lambda = 20$. The average network utility under the BNE, 'All FD', and random schemes decreases with $\chi_{\max}$ due to the increase in the residual self-interference signal. However, the average network utility is constant with $\chi_{\max}$ for the 'All HD' scheme. As shown in Figure 21, the BNE returns the maximum sum utilities for the whole network. Note also that at low $\chi_{\max}$, the 'All FD' strategy dominates the 'All HD' strategy since with good SIC capabilities, the amount of residual self-interference is very low. As $\chi_{\max}$ increases, the average network utility under the 'All FD' strategy decreases, which makes the 'All HD' strategy dominates the 'All FD' and the random strategies. Furthermore, we found that under the BNE and at $\lambda = 20$, the FD action occurs less frequently as $\chi_{\max}$ increases, while that of the HD increases in occurrence as shown in Figure 22.

Figure 23 shows the average network utility versus $\chi_{\max}$ at $\lambda = 70$. At high network density, external interference is more dominant than residual self-interference. This trend remains until a certain point at which nodes' SIC capabilities become very low (i.e., $\chi_{\max}$ is very high). Under the BNE scheme, the HD action is more frequent than the FD action for all values of $\chi_{\max}$, as shown in Figure 24. The reason for this behavior is that the network is very dense (i.e., $\lambda = 70$), hence the HD action is more favorable. Figure 25 shows the average per-link utility versus λ at $\chi_{\max} = 2 \times 10^{-4}$ for the four schemes. As the network density increases, the average per-link utility decreases due to the increase in the external interference. Since $\chi_{\max}$ is relatively high, the 'All HD' scheme outperforms the 'All FD' scheme. The average per-link utility under the BNE outperforms the other schemes.

7 Conclusions and Future Research

In this paper, we developed a novel Bayesian game-theoretic framework to study the coexistence problem between two FD-capable wireless links, where nodes have heterogeneous SIC capabilities. Although the throughput of a single link enhances significantly when operating in the FD mode, the additional interference caused (compared to the HD case) may limit its coexistence with a neighboring link. Our analysis revealed that the SIC capability of each link (which is the type of each player) has a double-threshold structure, i.e., the range of the SIC values can be divided into three regions. When the SIC capability is very good, operating in the FD mode strictly dominates the HD mode, whereas when the SIC capability is very poor, operating in the HD mode strictly dominates the FD mode. When the SIC capability is in the middle region, we derived the conditions on the probability distribution of the types of the other link under which HD (FD) strictly dominates FD (HD).

Our results corroborated that FD is not always the optimal mode when considering an FD-enabled wireless network. The optimal mode of a link depends on (i) the external interference it encounters from neighboring links (which is a function of their transmission powers and channel gains) and (ii) its residual self-interference (which is a function of its SIC capability, its transmission power, and its channel gain). Given that the external interference will not be known a priori, a link relies on the probability distribution over the types of the other link in deriving its strategy. Our simulations demonstrated the impact of the residual self-interference and external interference on the BER.

To capture the interaction between more than two links, we studied the coexistence problem in a network setting, where multiple FD-enabled links with heterogeneous SIC capabilities are collocated in the same region. Specifically, we focused on the case where every player is mainly affected by a single dominating link. Under this assumption, we showed that different games in the network do not involve more than two players. In our network simulations, which is based on PPP, we showed that the network sum utility under the derived BNE outperforms other traditional schemes (e.g., all players play FD, HD, or flip a coin to select the action). We also studied the effect of the network density and players' SIC on players' sum utilities.

Different directions of future research exist. First, we will design practical distributed algorithms that enable multiple links to converge to the BNE without the need of a centralized node. Furthermore, we will investigate the optimization of the distributed algorithm to minimize the convergence time while maintaining low control overhead between nodes. Second, we will investigate a power control scheme to be used as part of the game, in addition to FD/HD mode selection. In this case, an additional dimension will be added to the game, where each player needs to select the optimal action (FD or HD) and the transmission power in each case.

Acknowledgement

The work of M. Krunz was supported by the National Science Foundation (grants # IIP-1265960, CNS-1563655, and IIP-1535573). Any opinions, findings, conclusions, or recommendations expressed in this paper are those of the author(s) and do not necessarily reflect the views of NSF.

REFERENCES

[1] W. Afifi, M. J. Abdel-Rahman, M. Krunz, and A. B. MacKenzie, "Coexistence in wireless networks with heterogeneous self-interference cancellation capabilities," in *Proceedings of the International Symposium on Modeling and Optimization in Mobile, Ad Hoc, and Wireless Networks (WiOpt)*, May 2016.

[2] Z. Zhang, X. Chai, K. Long, A. V. Vasilakos, and L. Hanzo, "Full duplex techniques for 5G networks: Self-interference cancellation, protocol design, and relay selection," *IEEE Communications Magazine*, vol. 53, no. 5, pp. 128–137, 2015.

[3] D. Kim, H. Lee, and D. Hong, "A survey of in-band full-duplex transmission: From the perspective of PHY and MAC layers," *IEEE Communications Surveys & Tutorials*, vol. 17, no. 4, pp. 2017–2046, 2015.

[4] A. Sabharwal, P. Schniter, D. Guo, D. W. Bliss, S. Rangarajan, and R. Wichman, "In-band full-duplex wireless: Challenges and opportunities," *IEEE Journal on Selected Areas in Communications*, vol. 32, no. 9, pp. 1637–1652, September 2014.

[5] D. Bharadia, E. McMilin, and S. Katti, "Full duplex radios," in *Proceedings of the ACM SIGCOMM Conference*, 2013, pp. 375–386.

[6] M. J. Abdel-Rahman, M. AbdelRaheem, and A. B. MacKenzie, "Stochastic resource allocation in opportunistic LTE-A networks with heterogeneous self-interference cancellation capabilities," in *Proceedings of the IEEE DySPAN Conference*, 2015, pp. 200–208.

[7] W. Afifi, M. Hassan, and M. Krunz, "Enabling media streaming over LTE-U small cells," in *Proc. of the IEEE WCNC'16 Conf.*, April 2016, pp. 1–6.

[8] J. I. Choi, M. Jain, K. Srinivasan, P. Levis, and S. Katti, "Achieving single channel, full duplex wireless communication," in *Proc. of the ACM Mobicom'10 Conf.*, Chicago, Illinois, Sep. 2010, pp. 1 – 12.

[9] M. Duarte and A. Sabharwal, "Full-duplex wireless communications using off-the-shelf radios: Feasibility and first results," in *Proceedings of the IEEE ASILOMAR Conference*, 2010, pp. 1558–1562.

[10] B. Radunovic, D. Gunawardena, P. Key, A. Proutiere, N. Singh, V. Balan, and G. Dejean, "Rethinking indoor wireless mesh design: Low power, low frequency, full-duplex," in *Proc. of the Fifth IEEE Workshop on Wireless Mesh Networks*, Boston, Massachusetts, Jun. 2010, pp. 1 – 6.

[11] M. Jain, J. I. Choi, T. Kim, D. Bharadia, S. Seth, K. Srinivasan, P. Levis, S. Katti, and P. Sinha, "Practical, real-time, full duplex wireless," in *Proc. of the ACM Mobicom'11 Conf.*, Las Vegas, Nevada, Sep. 2011, pp. 301 – 312.

[12] A. Sahai, G. Patel, and A. Sabharwal, "Pushing the limits of full-duplex: Design and real-time implementation," *Technical Report TREE1104, Rice University*, Feb. 2011.

[13] M. Duarte, C. Dick, and A. Sabharwal, "Experiment-driven characterization of full-duplex wireless systems," *IEEE Transactions on Wireless Communications*, vol. 11, no. 12, pp. 4296 – 4307, Dec. 2012.

[14] C. Psomas and I. Krikidis, "Outage analysis of full-duplex architectures in cellular networks," in *Proc. of the IEEE 81st Vehicular Technology Conference (VTC Spring)*. IEEE, 2015, pp. 1–5.

[15] X. Qin, H. Zeng, X. Yuan, B. Jalaian, Y. T. Hou, W. Lou, and S. Midkiff, "Impact of full duplex scheduling on end-to-end throughput in multi-hop wireless networks," *IEEE Transactions on Mobile Computing*, 2016.

[16] M. A. A. Khojastepour, K. Sundaresan, S. Rangarajan, and M. Farajzadeh-Tehrani, "Scaling wireless full-duplex in multi-cell networks," in *Proc. of the IEEE INFOCOM'15 Conf.* IEEE, 2015, pp. 1751–1759.

[17] X. Xie and X. Zhang, "Does full-duplex double the capacity of wireless networks?" in *Proceedings of the IEEE INFOCOM Conference*, 2014, pp. 253–261.

[18] M. Duarte, A. Sabharwal, V. Aggarwal, R. Jana, K. Ramakrishnan, C. W. Rice, and N. Shankaranarayanan, "Design and characterization of a full-duplex multiantenna system for WiFi networks," *IEEE Transactions on Vehicular Technology*, vol. 63, no. 3, pp. 1160–1177, 2014.

[19] Y. Yang, B. Chen, K. Srinivasan, and N. B. Shroff, "Characterizing the achievable throughput in wireless networks with two active RF chains," in *Proceedings of the IEEE INFOCOM Conference*, 2014, pp. 262–270.

[20] C. Nam, C. Joo, N. B. Shroff, and S. Bahk, "Power allocation with inter-node interference in full-duplex wireless OFDM networks," Tech. Rep., 2014. [Online]. Available: http://netlab.snu.ac.kr/~cwnam/PowerControl.pdf

[21] D. N. Nguyen and M. Krunz, "Be responsible: A novel communications scheme for full-duplex MIMO radios," in *Proceedings of the IEEE INFOCOM Conference*, 2015, pp. 1733–1741.

[22] L. Song, Y. Li, and Z. Han, "Game-theoretic resource allocation for full-duplex communications," *IEEE Wireless Communications*, vol. 23, no. 3, pp. 50–56, Jun. 2016.

[23] G. Liu, F. R. Yu, H. Ji, and V. C. M. Leung, "Virtual resource management in green cellular networks with shared full-duplex relaying and wireless virtualization: A game-based approach," *IEEE Transactions on Vehicular Technology*, vol. 65, no. 9, pp. 7529–7542, Sep. 2016.

[24] Y. Zhang, C. Guo, and W. Li, "Cooperative interference game in cognitive radio hidden terminal scenario," *China Communications*, vol. 12, no. 10, pp. 128–135, Oct. 2015.

[25] M. Al-Imari, M. Ghoraishi, P. Xiao, and R. Tafazolli, "Game theory based radio resource allocation for full-duplex systems," in *Proc. of the IEEE VTC Spring Conf.*, May 2015, pp. 1–5.

[26] C. Yao, K. Yang, L. Song, and Y. Li, "X-Duplex: Adapting of full-duplex and half-duplex," in *Proc. of the IEEE INFOCOM WKSHPS*, April 2015, pp. 55–56.

[27] H. A. Suraweera, I. Krikidis, G. Zheng, C. Yuen, and P. J. Smith, "Low-complexity end-to-end performance optimization in MIMO full-duplex relay systems," *IEEE Transactions on Wireless Communications*, vol. 13, no. 2, pp. 913–927, 2014.

[28] M.-M. Zhao, Y. Cai, Q. Shi, M. Hong, and B. Champagne, "Joint transceiver designs for full-duplex k-pair MIMO interference channel with SWIPT," *IEEE Transactions on Communications*, vol. 65, no. 2, pp. 890–905, 2017.

[29] W. Afifi and M. Krunz, "Exploiting self-interference suppression for improved spectrum awareness/efficiency in cognitive radio systems," in *Proc. of the IEEE INFOCOM'13 Conf.*, Turin, Italy, Apr. 2013, pp. 1258–1266.

[30] W. Afifi and M. Krunz, "Incorporating self-interference suppression for full-duplex operation in opportunistic spectrum access systems," *IEEE Transactions on Wireless Communications*, vol. 14, no. 4, pp. 2180–2191, April 2015.

[31] N. Tang, S. Mao, and S. Kompella, "Power control in full duplex underlay cognitive radio networks," *Elsevier Ad Hoc Networks Journal*, vol. 37, no. 2, pp. 183–194, Feb. 2016.

[32] M. Feng, S. Mao, and T. Jiang, "Joint duplex mode selection, channel allocation, and power control for full-duplex cognitive femtocell networks," *Elsevier Digital Communications and Networks Journal*, vol. 1, no. 1, pp. 30–44, Feb. 2015.

[33] M. J. Abdel-Rahman, M. AbdelRaheem, A. B. MacKenzie, K. Cardoso, and M. Krunz, "On the orchestration of robust virtual LTE-U networks from hybrid half/full-duplex Wi-Fi APs," in *Proceedings of the IEEE WCNC Conference*, 2016.

[34] S. Wang, V. Venkateswaran, and X. Zhang, "Exploring full-duplex gains in multi-cell wireless networks: A spatial stochastic framework," in *Proc. of the IEEE INFOCOM'15 Conf.*, 2015, pp. 855–863.

[35] X. Wang, H. Huang, and T. Hwang, "On the capacity gain from full duplex communications in a large scale wireless network," *IEEE Transactions on Mobile Computing*, vol. PP, no. 99, pp. 1–1, 2015.

[36] P. Madhusudhanan, J. G. Restrepo, Y. Liu, T. X. Brown, and K. R. Baker, "Downlink performance analysis for a generalized shotgun cellular system," *IEEE Transactions on Wireless Communications*, vol. 13, no. 12, pp. 6684–6696, Dec 2014.

[37] J. Schloemann, H. S. Dhillon, and R. M. Buehrer, "Toward a tractable analysis of localization fundamentals in cellular networks," *IEEE Transactions on Wireless Communications*, vol. 15, no. 3, pp. 1768–1782, March 2016.

Wessam Afifi is currently a Senior Research and Development Engineer at Mavenir Systems in Richardson, Texas. He received his PhD degree from the Electrical and Computer Engineering Department at the University of Arizona in 2016. He received the B.Sc. degree in Electrical Engineering from Alexandria University, Egypt, in 2009 and the M.Sc. degree in Communications and Information Technology from the Wireless Intelligent Networks Center (WINC), Nile University, Egypt, in 2011. In 2015, he was a wireless systems intern with Nokia Bell Labs, San Francisco. He is a co-inventor of seven US patent applications. Dr. Afifi's research interest is in the areas of wireless communications and networking, with emphasis on resource allocations, adaptive protocols, dynamic spectrum access systems, shared spectrum, and full-duplex communications. He won the first place in the graduate division of the physical sciences, Math., Computer Engineering and Computer Science category for the student showcase in Nov. 2014. In Jan. 2015, he won the GPSC Research and Project Grant. He won two best-poster awards at BWAC I/UCRCs in Apr. 2013 and Apr. 2016. He served as a TPC member for WCNC'16,'17, and VTC'17 and as a reviewer for many conferences and journals.

Mohammad J. Abdel-Rahman (S'12, M'15) is an Assistant Professor in the School of Computer Engineering and Informatics at Al Hussein Technical University (HTU), Amman, Jordan. Before joining HTU, he was a Research Associate in the Department of Electrical and Computer Engineering at Virginia Polytechnic Institute and State University. He received his PhD degree from the Electrical and Computer Engineering Department at the University of Arizona in 2014. Dr. Abdel-Rahman's research is in the broad area of wireless communications and networking, with particular emphasis on resource management, adaptive protocols, and security issues. He serves as a reviewer for several international conferences and journals. He is a member of the IEEE.

Marwan Krunz (S'93, M'95, SM'04, F'10) is the Kenneth VonBehren Endowed Professor in the Department of ECE at the University of Arizona. He also holds a joint appointment as a professor of computer science, and is the site co-director of the Broadband Wireless Access and Applications Center, a multi-university industry-focused NSF center with 16+ affiliated members from industry and DoD labs. He previously served as the UA site director for Connection One, an NSF IUCRC that focuses on wireless communication circuits and systems. He is an IEEE Fellow, an Arizona Engineering Faculty Fellow (2011-2014), and an IEEE Communications Society Distinguished Lecturer (2013 and 2014). He was the recipient of the 2012 IEEE TCCC Outstanding Service Award. He received the NSF CAREER award in 1998. In 2010, he was a Visiting Chair of Excellence Catedra de Excelencia" at the University of Carlos III de Madrid (Spain). In summer 2011, he was received a Fulbright Senior Specialist award, visiting with the University of Jordan, King Abdullah II School of Information Technology. He held numerous other short-term research positions in the US, Europe, and Australia. Dr. Krunzs research interests lie in the areas of wireless communications and networking, with emphasis on resource management, adaptive protocols, and security issues. He has published more than 250 journal articles and peer-reviewed conference papers, and is a co-inventor on several US patents. Since January 2017, he is the Editor-in-Chief (EIC) for the IEEE Transactions on Mobile Computing. He also serves on the editorial board for the IEEE Transactions on Cognitive Communications and Networks. Previously, he served on the editorial boards for the IEEE/ACM Transactions on Networking, IEEE Transactions on Mobile Computing, IEEE Transactions on Network and Service Management, Computer Communications Journal, and IEEE Communications Interactive Magazine. He was the general vice-chair for WiOpt 2016 and general co-chair for WiSec'12. He was the TPC chair for WCNC 2016 (Networking Track), INFOCOM'04, SECON'05, WoWMoM'06, and Hot Interconnects 9. He has served and continues to serve on the steering and advisory committees of numerous conferences and on the panels of several funding agencies. He was a keynote speaker, an invited panelist, and a tutorial presenter at many international conferences.

Allen B. MacKenzie (SM) is an Associate Professor in the Bradley Department of Electrical and Computer Engineering at Virginia Tech, where he has been on the faculty since 2003. He is the associate director of Wireless @ Virginia Tech. During the 2012-2013 academic year, he was an E. T. S. Walton Visiting Professor at Trinity College Dublin.

Prof. MacKenzie's research focuses on wireless communications systems and networks. His current research interests include cognitive radio and cognitive network algorithms, architectures, and protocols and the analysis of such systems and networks using game theory and stochastic optimization. His past and current research sponsors include the National Science Foundation, Science Foundation Ireland, the Defense Advanced Research Projects Agency, and the National Institute of Justice.

Prof. MacKenzie is a senior member of the IEEE and a member of the ASEE and the ACM. Prof. MacKenzie is an area editor of the *IEEE Transactions on Communications* and an associate editor of the *IEEE Transactions on Cognitive Communications and Networking*. He is the author of more than 90 refereed conference and journal papers and a co-author of the book *Game Theory for Wireless Engineers*.